

---

# Neural Path Features and Neural Path Kernel : Understanding the role of gates in deep learning

---

## Abstract

Rectified linear unit (ReLU) activations can also be thought of as *gates*, which, either pass or stop their pre-activation input when they are *on* (when the pre-activation input is positive) or *off* (when the pre-activation input is negative) respectively. A deep neural network (DNN) with ReLU activations has many gates, and the on/off status of each gate changes across input examples as well as network weights. For a given input example, only a subset of gates are *active*, i.e., on, and the sub-network of weights connected to these active gates is responsible for producing the output. At randomised initialisation, the active sub-network corresponding to a given input example is random. During training, as the weights are learnt, the active sub-networks are also learnt, and potentially hold very valuable information.

In this paper, we analytically characterise the role of active sub-networks in deep learning. To this end, we encode the on/off state of the gates of a given input in a novel *neural path feature* (NPF), and the weights of the DNN are encoded in a novel *neural path value* (NPV). Further, we show that the output of network is indeed the inner product of NPF and NPV. The main result of the paper shows that the *neural path kernel* associated with the NPF is a fundamental quantity that characterises the information stored in the gates of a DNN. We show via experiments (on MNIST and CIFAR-10) that in standard DNNs with ReLU activations NPFs are learnt during training and such learning is key for generalisation. Furthermore, NPFs and NPVs can be learnt in two separate networks and such learning also generalises well in experiments. In our experiments, we observe that almost all the information learnt by a DNN with ReLU activations is stored in the gates - a novel observation that underscores the need to further investigate the role of gating in DNNs.

## 1 Introduction

We consider deep neural networks (DNNs) with rectified linear unit (ReLU) activations. A special property of ReLU activations is that it can be written as a product of its pre-activation input, say  $q \in \mathbb{R}$  and a gating signal,  $\gamma_r(q) = \mathbb{1}_{\{q>0\}}$ , i.e.,  $\chi_r(q) = q \cdot \gamma_r(q)$ . In what follows we call  $\chi_r$  as the ReLU activation and  $\gamma_r$  as the ReLU gate. While the weights remain the same across input examples, the 1/0 state of the gates (or simply gates) change across input examples. For each input example, there is a corresponding *active* sub-network consisting of those gates which are 1, and the weights which pass through such gates. This active sub-network can be said to hold the memory for a given input, i.e., only those weights that pass through such active gates contribute to the output. In this viewpoint, at random initialisation of the weights, for a given input example, a random sub-network is active and produces a random output. However, as the weights change during training (say via gradient descent), the gates change, and hence the active sub-networks corresponding to the various input examples also change. At the end of training, for each input example, there is a learned active sub-network, and produces a learned output. Thus, the gates of a trained DNN could potentially contain valuable information. In this paper, we study the role of the gates, and the dynamics of the

gates while training DNNs using gradient descent (GD). Our findings can be summarised in the following claims which we theoretically/experimentally justify in the paper:

Claim I (see Section 6): *Active sub-networks are fundamental entities in DNNs with ReLU activations.*

Claim II (see Section 5): *Learning of the active sub-networks during training is key for generalisation.*

Before we discuss “Claims I and II” in terms of the novel contributions in this paper in Section 1.2, we present the background of *neural tangent feature and kernel* (NTF and NTK) in Section 1.1.

**Notation:** We denote the set  $\{1, \dots, n\}$  by  $[n]$ . For  $x, y \in \mathbb{R}^m$ ,  $\langle x, y \rangle = x^\top y$ . The maximum and minimum eigenvalue of a real symmetric matrix  $A$  are denoted by  $\rho_{\max}(A)$  and  $\rho_{\min}(A)$ . We consider fully-connected DNNs with  $w$  hidden units per layer and  $d - 1$  hidden layers. The output of the DNN for an input  $x \in \mathbb{R}^{d_{in}}$  is denoted by  $\hat{y}_\Theta(x) \in \mathbb{R}$ , where  $\Theta \in \mathbb{R}^{d_{net}}$  are the network weight ( $d_{net} = d_{in}w + (d - 2)w^2 + w$ ). We denote by  $\Theta(l, j, i)$ , the weight connecting the  $j^{th}$  hidden unit of layer  $l - 1$  to the  $i^{th}$  hidden unit of layer  $l \in [d]$ .  $\Theta(1) \in \mathbb{R}^{w \times d_{in}}$ ,  $\Theta(l) \in \mathbb{R}^{w \times w}$ ,  $\forall l \in \{2, \dots, d - 1\}$ ,  $\Theta(d) \in \mathbb{R}^{w \times 1}$ . The dataset is given by  $(x_s, y_s)_{s=1}^n \in \mathbb{R}^{d_{in}} \times \mathbb{R}$ . The loss function is given by  $L_\Theta = \frac{1}{2} \sum_{s=1}^n (\hat{y}_\Theta(x_s) - y_s)^2$ . We use  $\nabla_\Theta(\cdot)$  stands for the gradient of  $(\cdot)$  with respect to the network weights. We use vectorised notations  $y = (y_s, s \in [n])$ ,  $\hat{y}_\Theta = (\hat{y}_\Theta(x_s), s \in [n]) \in \mathbb{R}^n$  for the true and predicted outputs and  $e_t = (\hat{y}_{\Theta_t} - y) \in \mathbb{R}^n$  for the error in the prediction. We use  $\theta \in \Theta$  to denote single arbitrary weight, and  $\partial_\theta(\cdot)$  to denote  $\frac{\partial(\cdot)}{\partial\theta}$ .  $\Sigma \in \mathbb{R}^{n \times n}$  is the input Gram matrix with entries  $\Sigma(s, s') = \langle x_s, x_{s'} \rangle$ .

## 1.1 Background: Neural Tangent Feature and Kernel

The NTF and NTK machinery was developed in some of the recent works [9, 1, 4, 6] to understand optimisation and generalisation in DNNs trained using GD. For an input  $x \in \mathbb{R}^{d_{in}}$ , the NTF is given by  $\psi_{x, \Theta} = \nabla_\Theta \hat{y}_\Theta(x) \in \mathbb{R}^{d_{net}}$ , i.e., the gradient of the network output with respect to its weights. The NTK matrix on the dataset is the  $n \times n$  Gram matrix of the NTFs of the input examples, and is given by  $K_\Theta(s, s') = \langle \psi_{x_s, \Theta}, \psi_{x_{s'}, \Theta} \rangle$ ,  $s, s' \in [n]$ .

**Proposition 1.1 (Lemma 3.1 Arora et al. [2019]).** *Consider the GD procedure to minimise the squared loss  $L(\Theta)$  the infinitesimally small step-size:  $\dot{\Theta}_t = -\nabla_\Theta L_{\Theta_t}$ . It follows that the dynamics of the error term can be written as  $\dot{e}_t = -K_{\Theta_t} e_t$ .*

**Prior works** [9, 6, 1, 4] have studied DNNs trained using GD in the so called ‘NTK regime’, which occurs under appropriate randomised initialisation, and when the width of the DNN approaches infinity. The characterising property of the NTK regime is that as  $w \rightarrow \infty$ ,  $K_{\Theta_0} \rightarrow K^{(d)}$ , and  $K_{\Theta_t} \approx K^{(d)}$ , where  $K^{(d)}$  (see (2) in Appendix A) is a deterministic matrix whose superscript  $(d)$  denotes the depth of the DNN. Arora et al. [2019] show that infinite width DNN trained using GD is equivalent to kernel regression with the limiting NTK matrix  $K^{(d)}$  (and hence enjoys the generalisation ability of the limiting NTK matrix  $K^{(d)}$ ). Further, Arora et al. [2019] propose a pure kernel method based on what they call the CNTK, which is the limiting NTK matrix  $K^{(d)}$  for an infinite width convolutional neural network (CNN). Cao and Gu [2019] show that in the NTK regime, a DNN is almost a linear learner with the random NTFs at initialisation, and showed a generalisation bound in the form of  $\tilde{\mathcal{O}} \left( d \cdot \sqrt{y^\top (K^{(d)})^{-1} y / n} \right)^1$ .

**Open Question:** Arora et al. [2019] report a 5% – 6% performance gain of finite width CNNs (which do not operate in the NTK regime) over the exact CNTKs corresponding to infinite width CNNs, and infer that the study of DNNs in the NTK regime cannot fully explain the success of practical neural networks yet. Can we explain the reason for the performance gain of CNNs over CNTK?

## 1.2 Our Contributions

To the best of our knowledge, we are the first to analytically characterise the role played by active sub-networks in deep learning as presented in the ‘Claims I and II’. The key contributions can be arranged into three landmarks as described below.

<sup>1</sup>  $a_t = \mathcal{O}(b_t)$  if  $\limsup_{t \rightarrow \infty} |a_t/b_t| < \infty$ , and  $\tilde{\mathcal{O}}(\cdot)$  is used to hide logarithmic factors in  $\mathcal{O}(\cdot)$ .

- The first step involves breaking a DNN into individual paths, and each path again into gates and weights. To this end, we encode the states of the gates in a novel *neural path feature* (NPF) and the weights in a novel *neural path value* (NPV) and express the output of the DNN as an inner product of NPF and NPV (see Section 2). In contrast to NTF/NTK which are *first-order* quantities (based on derivatives with respect to the weights), NPF and NPV are *zeroth-order* quantities. The kernel matrix associated to the NPFs namely the *neural path kernel* (NPK) matrix  $H_\Theta \in \mathbb{R}^{n \times n}$  has a special structure, i.e., it can be written as a *Hadamard* product of the input Gram matrix, and a correlation matrix  $\Lambda_\Theta \in \mathbb{R}^{n \times n}$ , whose entries  $\Lambda_\Theta(s, s')$  is equal to the total number of path in the sub-network that is active for both input examples  $s, s' \in [n]$ . With the  $\Lambda_\Theta$  matrix we reach our first landmark.

- Second step is to characterise performance of active sub-networks in a ‘stand alone’ manner. To this end, we consider a new idealised setting namely fixed NPF (FNPF) setting, wherein, the NPFs are fixed (i.e., held constant) and only the NPV is learnt via gradient descent. In this setting, we show that (see Theorem 5.1), in the limit of infinite width and under randomised initialisation the NTK converges to a matrix  $K_{\text{FNPF}}^{(d)} = \text{constant} \times H_{\text{FNPF}}$ , where  $H_{\text{FNPF}} \in \mathbb{R}^{n \times n}$  is the NPK matrix corresponding to the fixed NPFs. The  $K_{\text{FNPF}}^{(d)}$  matrix is different from the  $K^{(d)}$  matrix of Jacot et al. [2018], Arora et al. [2019], Cao and Gu [2019], which is a result of the freedom to initialise the NPV statistically independent of the fixed NPFs (see Assumption 5.1). With Theorem 5.1, we reach our second landmark, i.e. we justify “Claim I”, that active sub-networks are fundamental entities, which follows from the fact that  $H_{\text{FNPF}} = \Sigma \odot \Lambda_{\text{FNPF}}$ , where  $\Lambda_{\text{FNPF}}$  corresponds to the fixed NPFs.

- Third step is to show experimentally that sub-network learning happens in practice. We show that in finite width DNNs with ReLU activations, NPFs are learnt continuously during training, and such learning is key for generalisation. We observe that fixed NPFs obtained from the initial stages of training generalise poorly than CNTK (of Arora et al. [2019]), whereas, fixed NPFs obtained from later stages of training generalise better than CNTK and generalise as well as standard DNNs with ReLU. This throws light on the open question in Section 1.1, i.e., the difference between the NTK regime and the finite width DNNs is perhaps due to NPF learning. In finite width DNNs, NPFs are learnt during training and in the NTK regime no such feature learning happens during training (since  $K^{(d)}$  is fixed). This completes our final landmark namely justification of “Claim II”.

## 2 Neural Path Feature and Kernel: Encoding Gating Information

The gating property of the ReLU activation allows us to express the output of the network as a summation of the contribution of the individual paths, and paves a natural way to encode the 1/0 states of the gates *without loss of information*. The contribution of a path is the product of the signal in its input node, the ‘ $d$ ’ weights in the path and the ‘ $(d - 1)$ ’ gates in the path. For an input  $x \in \mathbb{R}^{d_{\text{in}}}$ , and parameter  $\Theta \in \mathbb{R}^{d_{\text{net}}}$ , we encode the gating information in a novel *neural path feature* (NPF),  $\phi_{x,\Theta} \in \mathbb{R}^P$  and the weights in a novel *neural path value* (NPV)  $v_\Theta \in \mathbb{R}^P$ , where,  $P = d_{\text{in}} w^{(d-1)}$  is the total number of paths. The NPF co-ordinate of a path is the product of the signal at its input node and the gates in the path. The NPV co-ordinate of a path is the product of the weights in the paths. By stacking the NPFs of all the input examples we obtain the NPF matrix as  $\Phi_\Theta = (\phi_{x_s,\Theta}, s \in [n]) \in \mathbb{R}^{P \times n}$ . Then the input-output relationship of a DNN in vector form is given by:

$$\hat{y}_\Theta = \Phi_\Theta^\top v_\Theta, \quad (1)$$

where the NPF matrix  $\Phi_\Theta$  can also be interpreted as the *hidden feature matrix* which along with  $v_\Theta$  is learnt during gradient descent on  $\Theta \in \mathbb{R}^{d_{\text{net}}}$ .

### 2.1 Paths, Neural Path Feature, Neural Path Value and Network Output

A path starts from an input node, passes through exactly one weight (and one hidden node) in each layer and ends at the output node. We have a total of  $P = d_{\text{in}} w^{(d-1)}$  paths. Let us say that an enumeration of the paths is given by  $[P] = \{1, \dots, P\}$ . Let  $\mathcal{I}_l: [P] \rightarrow [w], l = 0, \dots, d - 1$  provide the index of the hidden unit through which a path  $p$  passes in layer  $l$  (with the convention that  $\mathcal{I}_d(p) = 1, \forall p \in [P]$ ).

**Definition 2.1.** Let  $x \in \mathbb{R}^{d_{\text{in}}}$  be the input to the DNN. For this input,

(i) The activity of a path  $p$  is given by :  $A_\Theta(x, p) \stackrel{\text{def}}{=} \prod_{l=1}^{d-1} G_{x,\Theta}(l, \mathcal{I}_l(p))$ .

Input Layer	:	$z_{x,\Theta}(0)$	=	$x$
Pre-Activation	:	$q_{x,\Theta}(l, i)$	=	$\Theta(l, \cdot, i)^\top z_{x,\Theta}(l-1), l \in [d-1], i \in [w]$
Gating Values	:	$G_{x,\Theta}(l, i)$	=	$\gamma_r(q_{x,\Theta}(l, i)), l \in [d-1], i \in [w]$ , where $\gamma_r(q) = \mathbb{1}_{\{q>0\}}$
Hidden Layer	:	$z_{x,\Theta}(l, i)$	=	$\chi_r(q_{x,\Theta}(l, i)) = q_{x,\Theta}(l, i) \cdot G_{x,\Theta}(l, i), l \in [d-1], i \in [w]$
Final Output	:	$\hat{y}_\Theta(x)$	=	$\Theta(d)^\top z_{x,\Theta}(d-1)$

Table 1: DNN with ReLU activation. Here,  $x \in \mathbb{R}^{d_{in}}$  is the input to the DNN, and  $\hat{y}_\Theta(x)$  is the output, ‘ $q$ ’s are pre-activation inputs, ‘ $z$ ’s are output of the hidden layers, ‘ $G$ ’s are the gating values.  $l \in [d-1]$  is the index of the layer, and  $i \in [w]$  is the index of the hidden units in a layer.

(ii) The neural path feature (NPF) is given by :  $\phi_{x,\Theta} \stackrel{def}{=} (x(\mathcal{I}_0(p))A_\Theta(x_s, p), p \in [P]) \in \mathbb{R}^P$ .

(iii) The neural path value (NPV) if given by :  $v_\Theta \stackrel{def}{=} (\Pi_{l=1}^d \Theta(l, \mathcal{I}_{l-1}(p), \mathcal{I}_l(p)), p \in [P]) \in \mathbb{R}^P$ .

A path  $p$  is active if all the gates in the paths are on.

**Proposition 2.1.** The output of the network can be written as an inner product of the NPF and NPV, i.e.,  $\hat{y}_\Theta(x) = \langle \phi_{x,\Theta}, v_\Theta \rangle = \sum_{p \in [P]} x(\mathcal{I}_0(p))A_\Theta(x, p)v_\Theta(p)$ .

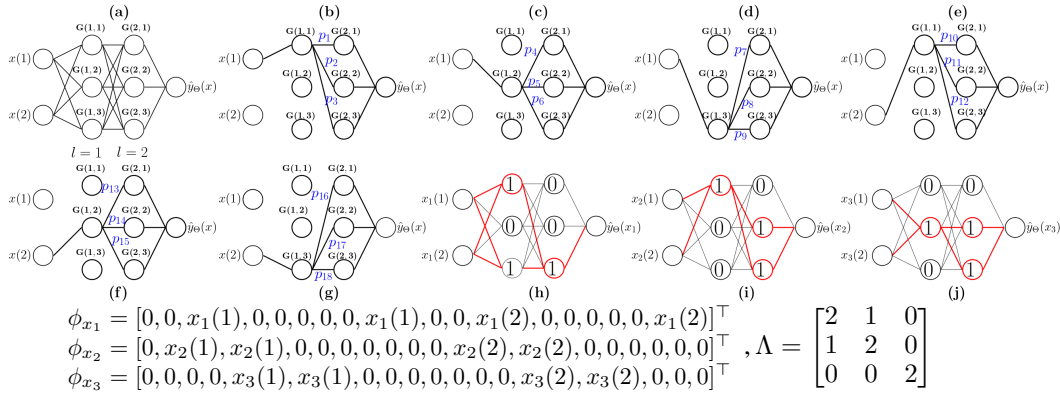


Figure 1: A toy illustration of gates, paths and active sub-networks. The cartoon (a) in the top left corner shows a DNN with 2 hidden layers, 6 ReLU gates  $G(l, i), l = 1, 2, i = 1, 2, 3, 2$  input nodes  $x(1)$  and  $x(2)$  and an output node  $\hat{y}_\Theta(x)$ . Cartoons (b) to (g) show the enumeration of the paths  $p_1, \dots, p_{18}$ . Cartoons (h), (i) and (j) show hypothetical gates for 3 different hypothetical input examples  $\{x_s\}_{s=1}^3 \in \mathbb{R}^2$ . In each of the cartoons (h), (i) and (j), the 1/0 inside the circles denotes the on/off state of the gates, and the bold paths/gates shown in red colour constitute the active sub-network for that particular input example. The NPFs are given by  $\phi_x = [x(1)A(x, p_1), \dots, x(1)A(x, p_9), x(2)A(x, p_{10}), \dots, x(2)A(x, p_{18})]^\top$ . Here,  $\Lambda(1, 2) = 1$  because paths  $p_3$  and  $p_{12}$  are both active for input examples  $x_1$  and  $x_2$  and the input dimension is 2.

## 2.2 Neural Path Kernel : Similarity based on active sub-networks

**Definition 2.2.** For an input examples  $s, s' \in [n]$ , define  $\mathcal{A}_\Theta(s, s') \stackrel{def}{=} \{p: A_\Theta(x_s, p) = 1, A_\Theta(x_{s'}, p), p \in [P]\}$  be the set of ‘active’ paths in the DNN, and  $\Lambda_\Theta(s, s') \stackrel{def}{=} \frac{|\mathcal{A}_\Theta(s, s')|}{d_{in}}$ .

**Remark:** Owing to the symmetry of a DNN, the same number of active paths start from any fixed input node. In Definition 2.2,  $\Lambda_\Theta$  measures the size of the active sub-network as the total number of paths active paths starting from any fixed input node. For a examples  $s, s' \in [n], s \neq s'$ ,  $\Lambda_\Theta(s, s)$  is equal to the size of the sub-network active for  $s$ , and  $\Lambda_\Theta(s, s')$  is equal to the size of the sub-network active for both  $s$  and  $s'$ . For an illustration of NPFs and  $\Lambda$  please see Figure 1.

**Lemma 2.1.** Let  $H_\Theta \stackrel{def}{=} \Phi_\Theta^\top \Phi_\Theta$  be the NPK matrix, and  $\Lambda_\Theta \in \mathbb{R}^{n \times n}$  be as in Definition 2.2. It follows that  $H_\Theta = \Sigma \odot \Lambda_\Theta$ , where  $\odot$  is the Hadamard product, and  $\Sigma$  is the input Gram matrix.

### 3 Dynamics of Gradient Descent with NPF and NPV Learning

In Section 2 we mentioned that during gradient descent, the DNN is learning a relation  $\hat{y}_\Theta = \Phi_\Theta^\top v_\Theta$ , i.e., both the NPFs and the NPV are learnt. In this section, we connect the newly defined quantities, i.e.,  $\Phi_\Theta$  and  $v_\Theta$  to the NTK matrix  $K_\Theta$  (see Proposition 3.1), and re-write the gradient descent dynamics in Proposition 3.2 taking into account of NPF and NPV learning.

#### 3.1 NPV and NPF Learning

**Definition 3.1.** The gradient of the NPV of path  $p$  is defined as  $\varphi_{p,\Theta} \stackrel{\text{def}}{=} (\partial_\theta v_\Theta(p), \theta \in \Theta) \in \mathbb{R}^{d_{\text{net}}}$ .

**Remark** The change of the NPV is given by  $\dot{v}_{\Theta_t}(p) = \langle \varphi_{p,\Theta_t}, \dot{\Theta}_t \rangle$ , where  $\dot{\Theta}_t$  is the change of the weights. We now collect the gradients  $\varphi_{p,\Theta}$  of all the paths to define a *value tangent kernel* (VTK).

**Definition 3.2.** Let  $\nabla_{\Theta} v_\Theta$  be a  $d_{\text{net}} \times P$  matrix of NPV derivatives given by  $\nabla_{\Theta} v_\Theta = (\varphi_{p,\Theta}, p \in [P])$ . Define the VTK to be the  $P \times P$  matrix given by  $\mathcal{V}_\Theta = (\nabla_{\Theta} v_\Theta)^\top (\nabla_{\Theta} v_\Theta)$ .

**Remark** An important point to note here is that the VTK is a quantity that is dependent only on the weights. To appreciate the same, consider a deep linear network (DLN) [15, 5] which has identity activations, i.e., all the gates are 1 for all inputs, and weights. For a DLN and DNN with identical network architecture (i.e.,  $w$  and  $d$ ), and identical weights,  $\mathcal{V}_\Theta$  is also identical. Thus,  $\mathcal{V}_\Theta$  is the gradient based information that excludes the gating information.

The NPFs changes at those time instants when any one of the gates switches from 1 to 0 or from 0 to 1. In the time between two such switching instances, NPFs of all the input examples in the dataset remain the same, and between successive switching instances, the NPF of at least one of the input example in the dataset changes. In what follows, in Proposition 3.2 we re-write Proposition 1.1 taking into account the switching instances which we define in Definition 3.3.

**Definition 3.3.** Define a sequence of monotonically increasing time instants  $\{T_i\}_{i=0}^\infty$  (with  $T_0 = 0$ ) to be ‘switching’ instants if  $\phi_{x_s,\Theta_t} = \phi_{x_s,\Theta_{T_i}}, \forall s \in [n], \forall t \in [T_i, T_{i+1}), i = 0, \dots, \infty$ , and  $\forall i = 0, \dots, \infty \exists s(i) \in [n]$  such that  $\phi_{x_{s(i)},\Theta_{T_i}} \neq \phi_{x_{s(i)},\Theta_{T_{i+1}}}$ .

#### 3.2 Gradient Descent

**Proposition 3.1.** The NTK is given by  $K_\Theta = \Phi_\Theta^\top \mathcal{V}_\Theta \Phi_\Theta$ .

**Remark**  $K_{\Theta_t}$  changes during training (i) continuously at all  $t \geq 0$  due to  $\mathcal{V}_{\Theta_t}$ , and (ii) at switching instants  $T_i, i = 0, \dots, \infty$  due to the change in  $\Phi_{\Theta_{T_i}}$ . We now describe the gradient descent dynamics taking into the dynamics of the NPV and the NPFs.

**Proposition 3.2.** Let  $\{T_i\}_{i=0}^\infty$  be as in Definition 3.3. For  $t \in [T_i, T_{i+1})$  and small step-size of GD:

$$\begin{aligned} \text{Weights Dynamics} &: \dot{\Theta}_t &= -\sum_{s=1}^n \psi_{x_s,\Theta_t} e_t(s) \\ \text{NPV Dynamics} &: \dot{v}_{\Theta_t}(p) &= \langle \varphi_{p,\Theta_t}, \dot{\Theta}_t \rangle, \forall p \in [P] \\ \text{Error Dynamics} &: \dot{e}_t &= -K_{\Theta_t} e_t, \text{ where } K_{\Theta_t} = \Phi_{\Theta_{T_i}}^\top \mathcal{V}_{\Theta_t} \Phi_{\Theta_{T_i}} \end{aligned}$$

**Proposition 3.3.**  $\rho_{\min}(K_\Theta) \leq \rho_{\min}(H_\Theta) \rho_{\max}(\mathcal{V}_\Theta)$ .

**Remark** For the NTK to be well conditioned, it is necessary for the NPK to be well conditioned. This is quite intuitive, in that, the closer two inputs are, the closer are their NPFs, and it is harder to train the network to produce arbitrarily different outputs for such inputs that are very close to one another.

### 4 Deep Gated Networks: Decoupling Neural Path Feature and Value

In order to ascertain that NPF learning indeed makes a difference, we should measure the generalisation performance with and without NPF learning. This can be achieved by a deep gated network (see Figure 2 below for details) having two networks of identical architecture namely i) a feature network parameterised by  $\Theta^F \in \mathbb{R}^{d_{\text{net}}}$ , that holds gating information, and hence the NPFs and

ii) a value network that holds the NPVs parameterised by  $\Theta^V \in \mathbb{R}^{d_{net}}$ . In what follows, we let  $\Theta^{DGN} = (\Theta^F, \Theta^V) \in \mathbb{R}^{2d_{net}}$  to denote the combined parameters of a DGN. By making  $\Theta^F \in \mathbb{R}^{d_{net}}$  trainable/non-trainable, we can *enable/disable* the NPF gradient, which gives rise to the following two modes of operating a DGN:

1. **Fixed NPF (FNPF):** Here,  $\Theta_t^F = \Theta_0^F, \forall t \geq 0$ , i.e.,  $\Theta^F \in \mathbb{R}^{d_{net}}$  is non-trainable. Thus the DGN learns the relation  $\hat{y}_{\Theta^{DGN}} = \Phi_{\Theta_0^F}^\top v_{\Theta^V}$ , where  $\Phi_{\Theta_0^F} \in \mathbb{R}^{P \times n}$  is a fixed NPF matrix, and  $v_{\Theta^V}$  is learned via gradient descent on  $\Theta^V \in \mathbb{R}^{d_{net}}$ .

2. **Decoupled NPF Learning (DNPFL):** Here both  $\Theta^F \in \mathbb{R}^{d_{net}}$  and  $\Theta^V \in \mathbb{R}^{d_{net}}$  are trained, and the DGN learns the relation  $\hat{y}_{\Theta^{DGN}} = \Phi_{\Theta^F}^\top v_{\Theta^V}$ . In comparison to (1), here we have two parameters  $\Theta^F \in \mathbb{R}^{d_{net}}$  and  $\Theta^V \in \mathbb{R}^{d_{net}}$  as opposed to a single  $\Theta \in \mathbb{R}^{d_{net}}$  in (1).

**Note:** FNPF and DNPFL are idealised modes to understand the role of gates, and not alternate proposals to replace standard DNNs with ReLU activations.

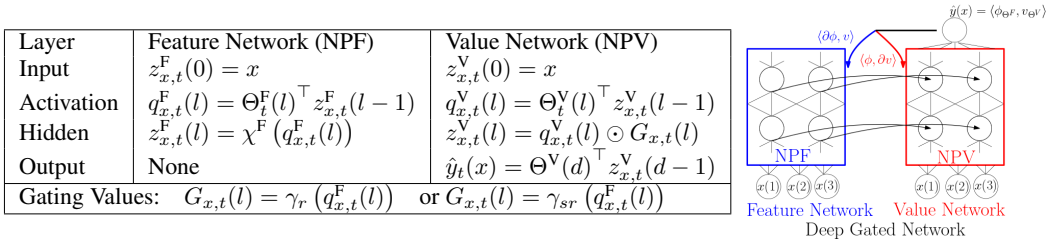


Figure 2: Deep gated network (DGN) setup. The pre-activations  $q_{x,t}^F(l)$  of layer  $l \in [d-1]$  from the feature network are used to derive the gating values  $G_{x,t}(l)$  of layer  $l \in [d-1]$ .

**Proposition 4.1** (Gradient Dynamics in a DGN). *Let  $\psi_{x,\Theta^{DGN}}^F \stackrel{def}{=} \nabla_{\Theta^F} \hat{y}_{\Theta^{DGN}}(x) \in \mathbb{R}^{d_{net}}$ ,  $\psi_{x,\Theta^{DGN}}^V \stackrel{def}{=} \nabla_{\Theta^V} \hat{y}_{\Theta^{DGN}}(x) \in \mathbb{R}^{d_{net}}$ . Let  $K_{\Theta^{DGN}}^V$  and  $K_{\Theta^{DGN}}^F$  be  $n \times n$  matrices with entries  $K_{\Theta^{DGN}}^V(s, s') = \langle \psi_{x_s, \Theta^{DGN}}^V, \psi_{x_{s'}, \Theta^{DGN}}^V \rangle$  and  $K_{\Theta^{DGN}}^F(s, s') = \langle \psi_{x_s, \Theta^{DGN}}^F, \psi_{x_{s'}, \Theta^{DGN}}^F \rangle$ . For infinitesimally small step-size of GD, the error dynamics in a DGN (in the DNPFL and FNPF modes) is given by:*

	DNPFL		FNPF
Weight	$\dot{\Theta}_t^V$	$= -\sum_{s=1}^n \psi_{x_s, \Theta_t^{DGN}}^V e_t(s), \dot{\Theta}_t^F = -\sum_{s=1}^n \psi_{x_s, \Theta_t^{DGN}}^F e_t(s)$	$\dot{\Theta}_t^V$ same as (DNPFL), $\dot{\Theta}_t^F = 0$
NPF	$\dot{\phi}_{x_s, \Theta_t^F}(p)$	$= x(\mathcal{I}_0(p)) \sum_{\theta^F \in \Theta^F} \partial_{\theta^F} A_{\Theta_t^F}(x_s, p) \dot{\theta}_t^F, \forall p \in [P], s \in [n]$	$\dot{\phi}_{x_s, \Theta_t^F}(p) = 0$
NPV	$\dot{v}_{\Theta_t^V}(p)$	$= \sum_{\theta^V \in \Theta^V} \partial_{\theta^V} v_{\Theta_t^V}(p) \dot{\theta}_t^V, \forall p \in [P]$	$\dot{v}_{\Theta_t^V}(p)$ same as DNPFL
Error	$\dot{e}_t$	$= -(K_{\Theta_t^{DGN}}^V + K_{\Theta_t^{DGN}}^F) e_t$	$\dot{e}_t = -(K_{\Theta_t^{DGN}}^V) e_t$

**Remark:** The gradient dynamics in a DGN specified in Proposition 4.1 is similar to the gradient dynamics in a DNN specified in Proposition 3.2. Important difference is that in a DGN there are  $2d_{net}$  parameters, and hence the NTF  $\psi_{x,\Theta} = (\psi_{x,\Theta}^F, \psi_{x,\Theta}^V) \in \mathbb{R}^{2d_{net}}$ , wherein,  $\psi_{x,\Theta^{DGN}}^V \in \mathbb{R}^{d_{net}}$  flows through the value network and  $\psi_{x,\Theta^{DGN}}^F \in \mathbb{R}^{d_{net}}$  flows through the feature network.

## 5 Learning with Fixed NPFs: Role Of Active Sub-Networks

In this section, we provide theoretical justification for ‘‘Claim I’’, i.e., the active sub-networks are fundamental entities in DNNs.

**Definition 5.1.** *Define the measure of information stored in the gates of a DNN with parameter  $\bar{\Theta} \in \mathbb{R}^{d_{net}}$  to be the generalisation performance of a DGN with identical architecture operated in the FNPF mode whose  $\Theta_0^F = \bar{\Theta}$  are non-trainable, and  $\Theta^V \in \mathbb{R}^{d_{net}}$  are trained.*

Consider a DNN parameterised by  $\bar{\Theta} \in \mathbb{R}^{d_{net}}$ . At randomised initialisation, we can obtain random NPFs  $\Phi_{\bar{\Theta}_0}$ , and after training for  $T$  epochs, and we can obtain learnt NPFs  $\Phi_{\bar{\Theta}_T}$ . Thus, while measuring information in the gates of this trained DNN, as per Definition 5.1, we are retaining  $\Phi_{\bar{\Theta}_T}$  by storing the weights as  $\Theta_0^F = \bar{\Theta}_T$  in the feature network, and discarding  $v_{\bar{\Theta}_T}$ , and re-training  $\Theta^V$ .

to learn a new relation  $\hat{y}_{\Theta^{\text{DGN}}} = \Phi_{\Theta^{\text{F}}}^{\top} v_{\Theta^{\text{V}}} = \Phi_{\Theta^{\text{T}}}^{\top} v_{\Theta^{\text{V}}}$ . Similarly, in the case of random NPFs we are learning the relation,  $\hat{y}_{\Theta^{\text{DGN}}} = \Phi_{\Theta^{\text{F}}}^{\top} v_{\Theta^{\text{V}}} = \Phi_{\Theta^{\text{O}}}^{\top} v_{\Theta^{\text{V}}}$ . In what follows, we use  $H_{\text{FNPF}}$  to refer to  $H_{\Theta^{\text{F}}}$ .

**Assumption 5.1.** (i)  $\Theta_0^{\text{V}} \in \mathbb{R}^{d_{\text{net}}}$  is statistically independent of the fixed NPFs (stored in  $\Theta_0^{\text{F}} \in \mathbb{R}^{d_{\text{net}}}$  of the feature network), (ii)  $\Theta_0^{\text{V}}$  are sampled i.i.d from symmetric Bernoulli over  $\{-\sigma, +\sigma\}$ .

**Theorem 5.1.** Under Assumption 5.1, as  $w \rightarrow \infty$ ,  $K_{\Theta_0^{\text{DGN}}} \rightarrow K_{\text{FNPF}}^{(d)} = d \cdot \sigma^{2(d-1)} H_{\text{FNPF}}$ .

• **Active Sub-Network:** From previous results Arora et al. [2019], it follows that as  $w \rightarrow \infty$ , the optimisation and generalisation properties of the fixed NPF learner can be tied down to the infinite width NTK of the FNPF learner  $K_{\text{FNPF}}^{(d)}$  and hence  $H_{\text{FNPF}}$  (treating  $d\sigma^{2(d-1)}$  as a scaling factor). We can further breakdown  $H_{\text{FNPF}} = \Sigma \odot \Lambda_{\text{FNPF}}$ , where  $\Lambda_{\text{FNPF}} = \Lambda_{\Theta^{\text{F}}}$ . This justifies ‘‘Claim I’’.

•  $K^{(d)}$  in prior works [9, 1, 4] essentially becomes  $K_{\text{FNPF}}^{(d)}$  under Assumption 5.1. To understand this, let us consider a DNN with weights  $\Theta \in \mathbb{R}^{d_{\text{net}}}$ . From [9, 1, 4] it follows that under randomised initialisation of  $\Theta_0 \in \mathbb{R}^{d_{\text{net}}}$  as  $w \rightarrow \infty$  the NTK of the DNN  $K_{\Theta_0} \rightarrow K^{(d)}$ . The simplification of  $K^{(d)}$  to  $K_{\text{FNPF}}^{(d)}$  in Theorem 5.1 occurs when we copy these random NPFs corresponding to  $\Theta_0 \in \mathbb{R}^{d_{\text{net}}}$  into the feature network and keep them fixed, i.e.,  $\Theta_t^{\text{F}} = \Theta_0^{\text{F}} = \Theta_0 \in \mathbb{R}^{d_{\text{net}}}, t \geq 0$ , and train  $\Theta^{\text{V}} \in \mathbb{R}^{d_{\text{net}}}$  with initialisation as per Assumption 5.1.

• **Choice of  $\sigma$ :** In the case of random NPFs obtained by initialising  $\Theta_0^{\text{F}}$  at random by sampling from a symmetric distribution, we expect  $\frac{w}{2}$  gates to be on every layer, so  $\sigma = \sqrt{\frac{2}{w}}$  is a normalising choice, in that, the diagonal entries of  $\sigma^{2(d-1)} \Lambda_{\text{FNPF}}(s, s) \approx 1$  in this case.

• We discuss a more detailed version of Theorem 5.1 in the Appendix, where we discuss the role of width and depth on a pure memorisation task.

## 6 Experiments: Fixed NPFs, NPF Learning and Verification of Claim II

In this section, we justify ‘‘Claim II’’, i.e., active sub-networks learning is key for generalisation. Since the active sub-network are encoded in the NPFs, we verify the claim by comparing different network settings which vary in their NPF learning capabilities. We resolve the open question of Arora et al. [2019] mentioned in Section 1.1, by providing an empirical explanation for the performance gain of finite width CNN over the pure kernel method based on the exact infinite width CNTK.

**Networks for Comparison:** The performance of the following networks on standard MNIST and CIFAR-10 datasets will be used for comparison: (i) fixed random (FRNPF): in the DGN, we randomly initialise both  $\Theta_0^{\text{F}}, \Theta_0^{\text{V}}$ , make  $\Theta^{\text{F}}$  *non-trainable* and train only  $\Theta^{\text{V}}$ , (ii) fixed learnt (FLNPF): we initialise  $\Theta_0^{\text{V}}$  randomly, and copy weights from a pre-trained ReLU network (of identical architecture) into  $\Theta_0^{\text{F}}$ . Similar to FR case,  $\Theta^{\text{F}}$  is non-trainable and only  $\Theta^{\text{V}}$  is trained (iii) decoupled learning (DNPFL): we randomly initialise both  $\Theta_0^{\text{F}}, \Theta_0^{\text{V}}$ , and train both  $\Theta^{\text{F}}$  and  $\Theta^{\text{V}}$ , (iv) ReLU: Standard DNNs/CNNs with ReLU. We will also use the numerical results reported in Arora et al. [2019].

**1. Finite Vs Infinite width alone is not enough to explain the performance gain of CNN:** Both FRNPF and ReLU are finite width networks. However, performance of FRNPF is approximately 67% which is worse than CNTK of Arora et al. [2019] whose performance is 77.43%, and the performance of our CNN architecture with *global-average-pooling* (GCONV in Table 2) is 80.34%. We trained FRNPF with independent initialisation (II), where  $\Theta_0^{\text{F}}$  and  $\Theta_0^{\text{V}}$  are statistically independent, and dependent initialisation (DI), where  $\Theta_0^{\text{F}} = \Theta_0^{\text{V}}$ . FRNPF (II) and FRNPF (DI) were close in our experiments (see columns 4 and 5 in Table 2). Further, both FRNPF (DI) and ReLU start with the same NTK matrix at initialisation. If finite width was the sole reason for the better performance then even FRNPF (II), (DI) should have performed better than CNTK in the experiments, and they did not. Thus, finite width alone does not explain the performance gain of CNN over CNTK.

**2. NPF Learning Vs No NPF Learning is key to explain the performance gain of CNN:** FLNPF with weights copied from a fully trained ReLU performs close to 79.68% which is almost as good as ReLU (80.43%). Further, NPFs are learnt continuously during the training, and the performance gap between FRNPF and ReLU is continuous. In the case of CIFAR-10, we trained a GCONV network (parameterised by  $\Theta$ ) for 60 epochs, and we obtained 6 different weights at various *stages* of the training process. Stage 1:  $\bar{\Theta}_{10}$ , stage 2:  $\bar{\Theta}_{20}$ , stage 3:  $\bar{\Theta}_{30}$ , stage 4:  $\bar{\Theta}_{40}$ , stage 5:  $\bar{\Theta}_{50}$ ,

stage 6:  $\bar{\Theta}_{60}$ . We copy these weights obtained at various stages of training to setup 6 different FLNPFs, i.e., FLNPF-1 to FLNPF-6. We observe that the performance of FLNPF-1 to FLNPF-6 increases monotonically, with FLNPF-1 performing 72% which is better than FRNPF (i.e., 67.08%), and FLNPF-6 performing as well as ReLU (see Figure 3). The performance of CNTK of Arora et al. [2019] is 77.43%. Thus, through its various stages, the FLNPF starts from below 77.43% and surpasses to reach 79.68%, which implies performance gain of CNN is due to learning of NPFs.

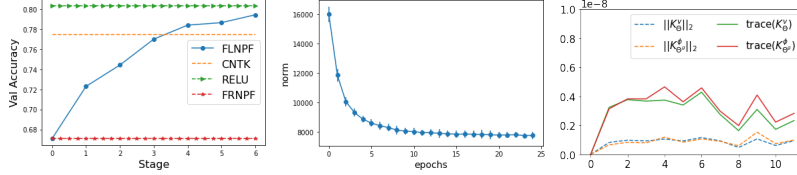


Figure 3: The left plot shows NPF learning with stages in  $x$ -axis and test accuracy in fraction in  $y$ -axis.

**3. Dynamics of active sub-networks during training:** We considered “Binary”-MNIST data set with two classes namely digits 4 and 7, with the labels taking values in  $\{-1, +1\}$  and squared loss. We trained a fully connected (FC) network ( $w = 100, d = 5$ ). Let  $\hat{H}_{\Theta_t} = \frac{1}{\text{trace}(H_{\Theta_t})} H_{\Theta_t}$  be the normalised NPK matrix. For a subset size,  $n' = 200$  (100 examples per class) we plot  $\nu_t = y^\top (\hat{H}_{\Theta_t})^{-1} y$ , (where  $y \in \{-1, 1\}^{200}$  is the labelling function), and observe that  $\nu_t$  reduces as training proceeds (see middle plot in Figure 3). Note that,  $\nu_t = \sum_{i=1}^{n'} (u_{i,t}^\top y)^2 (\hat{\rho}_{i,t})^{-1}$ , where  $u_{i,t} \in \mathbb{R}^{n'}$  are the orthonormal eigenvectors of  $\hat{H}_{\Theta_t}$  and  $\hat{\rho}_{i,t}, i \in [n']$  are the corresponding eigenvalues. Since  $\sum_{i=1}^{n'} \hat{\rho}_{i,t} = 1$ , the only way  $\nu_t$  reduces is when more and more energy gets concentrated on  $\hat{\rho}_{i,t}$ s for which  $(u_{i,t}^\top y)^2$ s are also high. Since  $H_{\Theta_t} = \Sigma \odot \Lambda_{\Theta_t}$ , only  $\Lambda_{\Theta_t}$  is learnt during training.

**4. Decoupled learning** of NPFs also performed better than FRNPFs (see column DNPFL in Table 2). This demonstrates the fact that NPFs can also be learnt in ‘stand alone’ manner. In this case, the NTK is given by  $K_{\Theta^{\text{DGN}}} = K_{\Theta^{\text{DGN}}}^V + K_{\Theta^{\text{DGN}}}^F$ . For MNIST, we compared  $K_{\Theta^{\text{DGN}}}^V$  and  $K_{\Theta^{\text{DGN}}}^F$  (calculated using 100 examples in total with 10 examples per each of the 10 classes) using their trace and Frobenius norms, and we observe that  $K_{\Theta^{\text{DGN}}}^V$  and  $K_{\Theta^{\text{DGN}}}^F$  are in the same scale, which is perhaps pointing to the fact that both  $K_{\Theta^{\text{DGN}}}^V$  and  $K_{\Theta^{\text{DGN}}}^F$  are equally important for obtaining good generalisation performance. In DNPFL, we can separately study the kernel  $K_{\Theta^{\text{DGN}}}^F$  responsible for NPF learning, an interesting future research direction.

## 7 Conclusion

In this paper, we studied the role of active sub-networks in deep learning by encoding the gates in the neural path features. We showed that neural path features are learnt during training and such learning is key for generalisation. In our experiments, we observed that almost all information of a trained DNN is stored in the neural path features. We conclude by saying *understanding deep learning requires understanding neural path feature learning*.

Arch	Optimiser	Dataset	FRNPF (II)	FRNPF (DI)	DNPFL	FLNPF	ReLU
FC	SGD	MNIST	95.85 $\pm$ 0.10	95.85 $\pm$ 0.17	97.86 $\pm$ 0.11	97.10 $\pm$ 0.09	97.85 $\pm$ 0.09
FC	Adam	MNIST	96.02 $\pm$ 0.13	96.09 $\pm$ 0.12	<b>98.22 <math>\pm</math> 0.05</b>	<b>97.82 <math>\pm</math> 0.02</b>	<b>98.14 <math>\pm</math> 0.07</b>
VCONV	SGD	CIFAR-10	58.92 $\pm$ 0.62	58.83 $\pm$ 0.27	63.21 $\pm$ 0.07	63.06 $\pm$ 0.73	67.02 $\pm$ 0.43
VCONV	Adam	CIFAR-10	64.86 $\pm$ 1.18	64.68 $\pm$ 0.84	<b>69.45 <math>\pm</math> 0.76</b>	<b>71.4 <math>\pm</math> 0.47</b>	<b>72.43 <math>\pm</math> 0.54</b>
GCONV	SGD	CIFAR-10	67.36 $\pm$ 0.56	66.86 $\pm$ 0.44	<b>74.57 <math>\pm</math> 0.43</b>	<b>78.52 <math>\pm</math> 0.39</b>	<b>78.90 <math>\pm</math> 0.37</b>
GCONV	Adam	CIFAR-10	67.09 $\pm$ 0.58	67.08 $\pm$ 0.27	<b>77.12 <math>\pm</math> 0.19</b>	<b>79.68 <math>\pm</math> 0.32</b>	<b>80.43 <math>\pm</math> 0.35</b>

Table 2: Shows the generalisation performance of different NPFs learning settings. The values in the table are averaged over 5 runs. Here, FC is a fully connected network with  $w = 100$  and  $d = 5$ . VCONV and GCONV denote Vanilla CNN and CNN with GAP respectively. Please check Appendix B for details on architecture of VCONV and GCONV, and the hyper-parameters.



## References

- [1] Sanjeev Arora, Simon S Du, Wei Hu, Zhiyuan Li, Russ R Salakhutdinov, and Ruosong Wang. On exact computation with an infinitely wide neural net. In *Advances in Neural Information Processing Systems*, pages 8139–8148, 2019.
- [2] Sanjeev Arora, Simon S Du, Wei Hu, Zhiyuan Li, and Ruosong Wang. Fine-grained analysis of optimization and generalization for overparameterized two-layer neural networks. *arXiv preprint arXiv:1901.08584*, 2019.
- [3] Randall Balestriero et al. A spline theory of deep learning. In *International Conference on Machine Learning*, pages 374–383, 2018.
- [4] Yuan Cao and Quanquan Gu. Generalization bounds of stochastic gradient descent for wide and deep neural networks. In *Advances in Neural Information Processing Systems*, pages 10835–10845, 2019.
- [5] Simon S Du and Wei Hu. Width provably matters in optimization for deep linear neural networks. *arXiv preprint arXiv:1901.08572*, 2019.
- [6] Simon S Du, Jason D Lee, Haochuan Li, Liwei Wang, and Xiyu Zhai. Gradient descent finds global minima of deep neural networks. *arXiv preprint arXiv:1811.03804*, 2018.
- [7] Jonathan Fiat, Eran Malach, and Shai Shalev-Shwartz. Decoupling gating from linearity. *CoRR*, abs/1906.05032, 2019. URL <http://arxiv.org/abs/1906.05032>.
- [8] Jonathan Frankle and Michael Carbin. The lottery ticket hypothesis: Finding sparse, trainable neural networks. *arXiv preprint arXiv:1803.03635*, 2018.
- [9] Arthur Jacot, Franck Gabriel, and Clément Hongler. Neural tangent kernel: Convergence and generalization in neural networks. In *Advances in neural information processing systems*, pages 8571–8580, 2018.
- [10] Arthur Jacot, Franck Gabriel, and Clément Hongler. Freeze and chaos for dnns: an ntk view of batch normalization, checkerboard and boundary effects. *arXiv preprint arXiv:1907.05715*, 2019.
- [11] Jaehoon Lee, Lechao Xiao, Samuel Schoenholz, Yasaman Bahri, Roman Novak, Jascha Sohl-Dickstein, and Jeffrey Pennington. Wide neural networks of any depth evolve as linear models under gradient descent. In *Advances in neural information processing systems*, pages 8570–8581, 2019.
- [12] Behnam Neyshabur, Russ R Salakhutdinov, and Nati Srebro. Path-sgd: Path-normalized optimization in deep neural networks. In *Advances in Neural Information Processing Systems*, pages 2422–2430, 2015.
- [13] Vivek Ramanujan, Mitchell Wortsman, Aniruddha Kembhavi, Ali Farhadi, and Mohammad Rastegari. What’s hidden in a randomly weighted neural network? *arXiv preprint arXiv:1911.13299*, 2019.
- [14] Andrew M Saxe, James L McClelland, and Surya Ganguli. Exact solutions to the nonlinear dynamics of learning in deep linear neural networks. *arXiv preprint arXiv:1312.6120*, 2013.
- [15] Ohad Shamir. Exponential convergence time of gradient descent for one-dimensional deep linear neural networks. In *Conference on Learning Theory*, pages 2691–2713, 2019.
- [16] Rupesh Kumar Srivastava, Jonathan Masci, Faustino Gomez, and Jürgen Schmidhuber. Understanding locally competitive networks. *arXiv preprint arXiv:1410.1165*, 2014.

## 8 Related Work

[10, 16, 3, 12, 2, 13, 8, 7, 14, 11]

### Appendix

#### A Expression for $K^{(d)}$

The  $K^{(d)}$  matrix is computed by the recursion in (2).

$$\begin{aligned}\tilde{K}^{(1)}(s, s') &= \Sigma^{(1)}(s, s') = \Sigma(s, s'), M_{ss'}^{(l)} = \begin{bmatrix} \Sigma^{(l)}(s, s) & \Sigma^{(l)}(s, s') \\ \Sigma^{(l)}(s', s) & \Sigma^{(l)}(s', s') \end{bmatrix} \in \mathbb{R}^2, \\ \Sigma^{(l+1)}(s, s') &= 2 \cdot \mathbb{E}_{(q, q') \sim N(0, M_{ss'}^{(l)})} [\chi(q)\chi(q')], \hat{\Sigma}^{(l+1)}(s, s') = 2 \cdot \mathbb{E}_{(q, q') \sim N(0, M_{ss'}^{(l)})} [\partial\chi(q)\partial\chi(q')], \\ \tilde{K}^{(l+1)} &= \tilde{K}^{(l)} \odot \hat{\Sigma}^{(l+1)} + \Sigma^{(l+1)}, K^{(d)} = (\tilde{K}^{(d)} + \Sigma^{(d)}) / 2\end{aligned}\tag{2}$$

where  $s, s' \in [n]$  are two input examples in the dataset,  $\Sigma$  is the data Gram matrix,  $\partial\chi$  stands for the derivative of the activation function with respect to the pre-activation input,  $N(0, M)$  stands for the mean-zero Gaussian distribution with co-variance matrix  $M$ .

#### B Experimental Setup

We used standard datasets namely MNIST and CIFAR-10, with categorical cross entropy loss. We used stochastic gradient descent (SGD) and *Adam*. In the case of SGD, we tried constant step-sizes in the set  $\{0.1, 0.01, 0.001\}$  and chose the best. In the case of Adam we used a constant step size of  $3e^{-4}$ . In both cases, we used batch size to be 32. We used a fully connected (FC) DNN with  $(w = 128, d = 6)$  for MNIST. To train CIFAR-10, we used *Vanilla-Convolutional* Network (VCONV) without pooling, residual connections, dropout or batch-normalisations, and is given by: input layer is  $(32, 32, 3)$ , followed by convolution layers with a stride of  $(3, 3)$  and channels 64, 64, 128, 128 followed by a flattening to layer with 256 hidden units, followed by a fully connected layer with 256 units, and finally a 10 width soft-max layer to produce the final predictions. To train CIFAR-10, we also used a GCONV which is same as VCONV with a *global-average-pooling* (GAP) layer. For both FRNPF, and FLNPF, we let  $\chi^F = \chi_r$ , and  $G_{x,t}(l) = \gamma_r(q_{x,t}^F(l))$ . In the case of FRNPF, we considered two possible initialisations namely i) *independent initialisation* (II), i.e.,  $\Theta_0^F$  and  $\Theta_0$  are statistically independent, and ii) *dependent initialisation* (DI), i.e.,  $\Theta_0^F = \Theta_0$ , a case which mimics the NPFs and NPVs of a standard DNN with ReLU activations. In the case of FLNPF,  $\Theta_0^F = \bar{\Theta}$ , where  $\bar{\Theta}$  is the parameter of a pre-trained (could be in various stages of training) DNN with ReLU activations. In the case, DNPFL, we let  $\chi^F = \chi_r$ , and  $G_{x,t}(l) = \gamma_{sr}(q_{x,t}^F(l))$  with  $\beta = 8$ . The use of soft-ReLU makes it straightforward for the feature gradients to flow via the gating network.

#### C Proofs of technical results